ELSEVIER

Volume 222, February 2015

CONTENTS

JOURNAL OF SOLID STATE CHEMISTRY

www.elsevier.com/locate/jssc

Abstracted/indexed in BioEngineering Abstracts, Chemical Abstracts, Coal Abstracts, Current Contents/Physics, Chemical, & Earth Sciences, Engineering Index, Research Alert, SCISEARCH, Science Abstracts, and Science Citation Index. Also covered in the abstract and citation database SCOPUS®. Full text available on ScienceDirect®.

Regular Articles

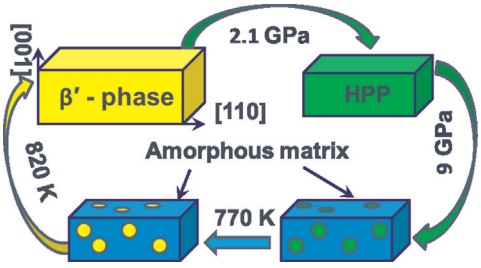

Schematic representation of pressure-induced amorphization and "memory glass" effect in rare-earth molybdate single crystals. The XRD and TEM measurements have revealed the presence of the residual identically oriented paracrystalline nanodomains in the pressure-amorphized state. These domains preserve the information about initial structure and orientation of the sample. They act as memory units and crystalline seeds during transformation of the amorphous phase back to the starting single crystalline one.

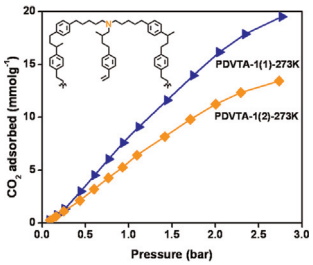

Exceptionally high CO_2 uptake (85.8 wt % at 273 K) has been observed over a high surface area porous organic polymer PDVTA-1 synthesized through copolymerization of divinylbenzene and triallyl amine.

Regular Articles—Continued

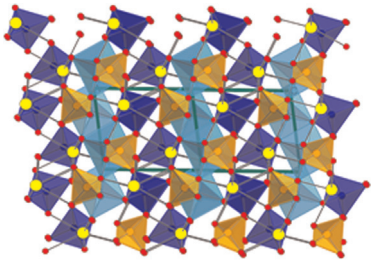

The crystal structure of $BiZn_2VO_6$, a new structure type in the BiM_2AO_6 (M=Mg, Ca, Cd, Cu, Pb, Mn, Zn; A=V, P, As) family.

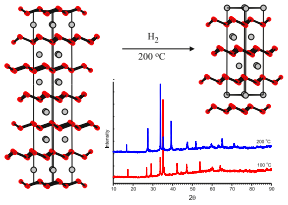

The common 6*R* form of $CaSi_2$ can be transformed quantitatively into 3*R*-$CaSi_2$ upon sintering in a hydrogen atmosphere.

Continued

Effects of the slab thickness on the crystal and electronic structures of $In_2O_3(ZnO)_m$ revealed by first-principles calculations

Jing Wen, Xitian Zhang and Hong Gao

page 25

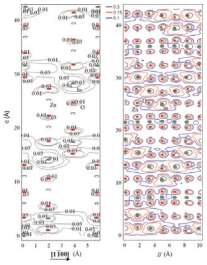

The conduction electrons are mainly distributed around the boundaries of the plane or zigzag shape. The optimized transport channels can be formed around the boundaries.

Conjugating folate on superparamagnetic Fe_3O_4@Au nanoparticles using click chemistry

Xiaofang Shen, Zhaoqiang Ge and Yuehong Pang

page 37

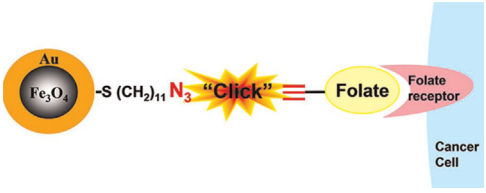

Self-assembled azide-terminated group on superparamagnetic Fe_3O_4@Au nanoparticles followed by click reaction with alkyne-functionalized folate, allowing the nanoparticles target folate receptor of cancer cells.

A cesium copper vanadyl-diphosphate: Synthesis, crystal structure and physical properties

Larisa Shvanskaya, Olga Yakubovich, Andrey Bychkov, Vasiliy Shcherbakov, Alexey Golovanov, Elena Zvereva, Olga Volkova and Alexander Vasiliev

page 44

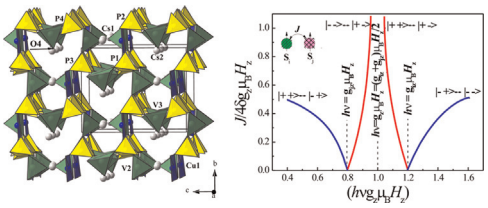

A microporous 3D anionic framework of the first copper vanadium-diphosphate $Cs_2Cu_{1.1}(VO)_{1.9}(P_2O_7)_2$. The similarity in behaviour of Cu and V paramagnetic subsystems revealed by ESR study.

Studies on the thermal stability of BiCuSeO

Celine Barreteau, David Berardan and Nita Dragoe

page 53

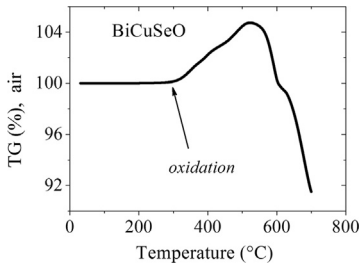

BiCuSeO oxidation under air, starting below 300 °C

Ba_2TeO: A new layered oxytelluride

T. Besara, D. Ramirez, J. Sun, J.B. Whalen, T.D. Tokumoto, S.A. McGill, D.J. Singh and T. Siegrist

page 60

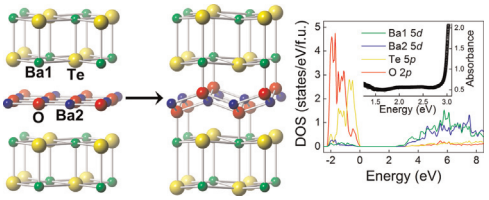

Starting from a simple stacking of rocksalt layers, the final structure of Ba_2TeO can be obtained by accommodation of structural strain via atom displacements. Density of states calculations and optical absorbance measurements show that Ba_2TeO has a band gap of 2.93 eV, indicative of semiconductor behavior.

Structure of β-$AgGaO_2$; ternary I–III–VI_2 oxide semiconductor with a wurtzite-derived structure

Hiraku Nagatani, Issei Suzuki, Masao Kita, Masahiko Tanaka, Yoshio Katsuya, Osami Sakata and Takahisa Omata

page 66

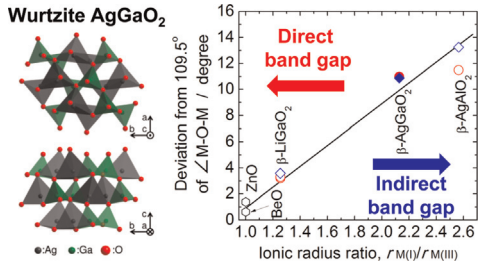

Crystal structure of β-$AgGaO_2$ was refined by Rietveld analysis. AgO_4 and $O(Ag,Ga)_4$ tetrahedra are significantly distorted from ideal tetrahedron.